

Supplementary material

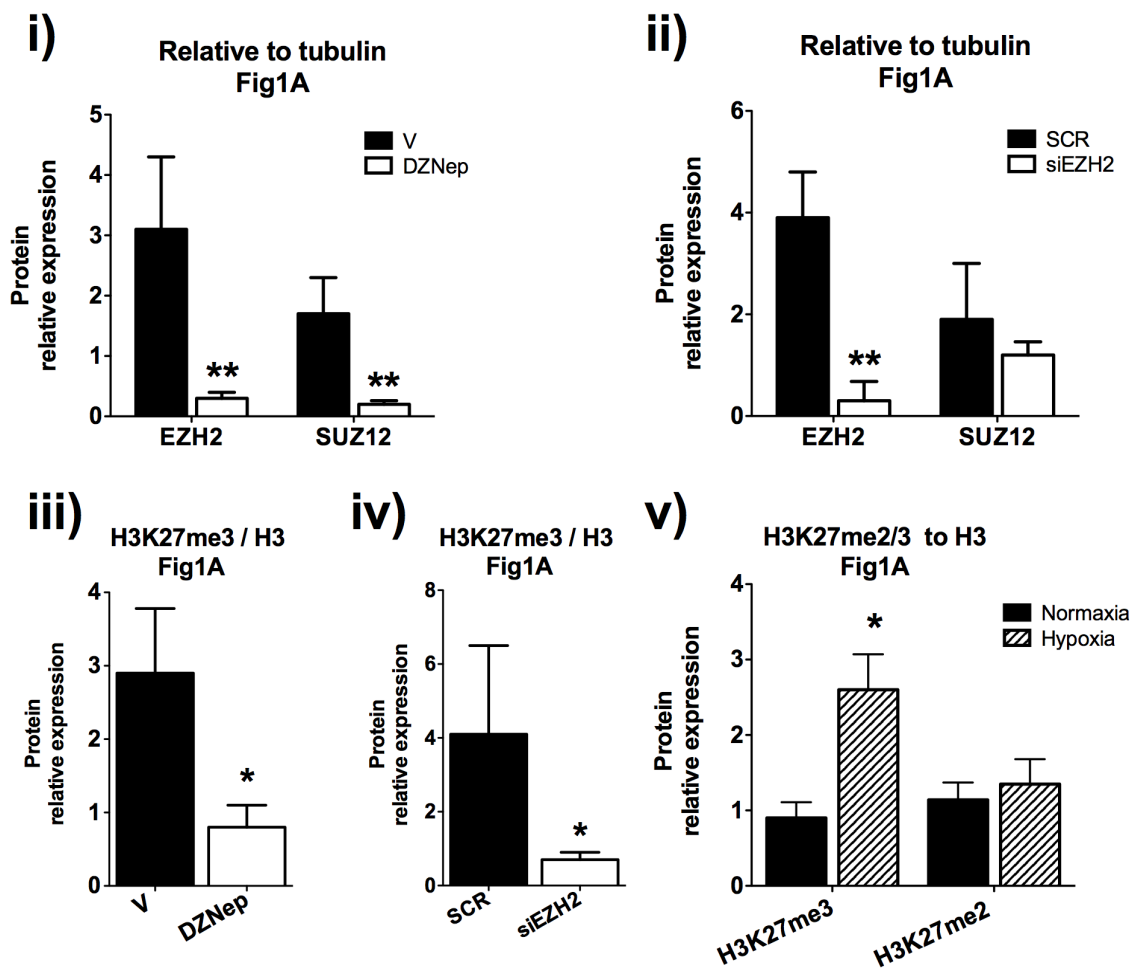


Figure S1. Quantification of Western blot analyses presented in the Figure 1A.

Data are presented as mean \pm SEM of minimum n=3 independent experiments. **p<0.01 and *p<0.05, vs. the respective control group (vehicle -V- for DZNep and scramble oligo sequence -SCR- for the small interfering RNA used to knock-down EZH2 -siEZH2).

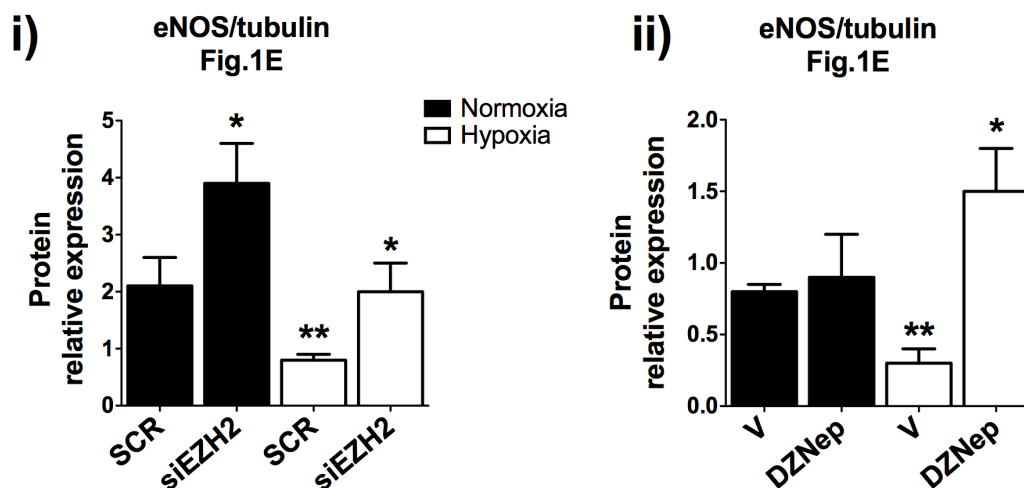


Figure S2. Quantification of Western blot analyses presented in the Figures 1E.

Data are presented as mean \pm SEM. ** $p < 0.01$ and * $p < 0.05$, vs. the respective control group (vehicle -V- for DZNep and scramble oligo sequence -SCR- for the small interfering RNA used to knock-down EZH2 -siEZH2) under normoxia, as mean of $n=3$ independent experiments.

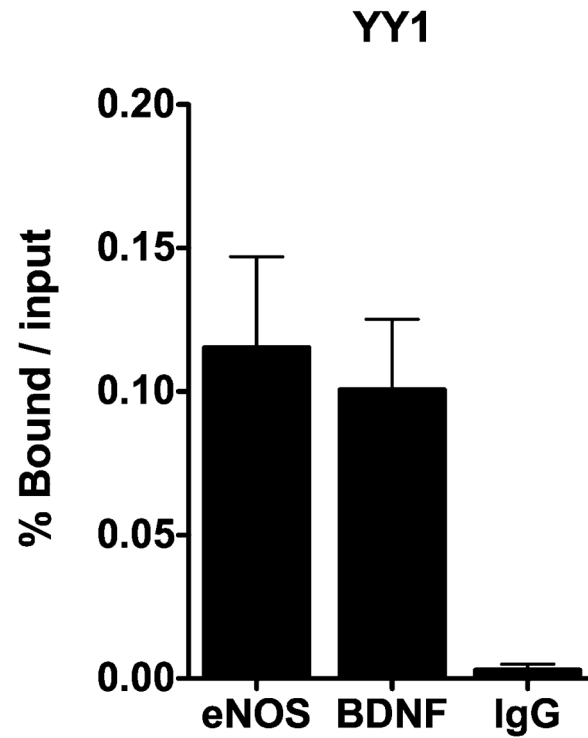


Figure S3. Binding of YY-1 to the eNOS and BDNF gene promoters.

Quantitative ChIP analysis of YY1 protein was performed in HUVECs to check its occupancy of locus on eNOS (-493/-318 bp) and BDNF (-753/-480 bp) within the promoter region. IgG was used as a negative control. Data were calculated as % bound/input. All data were expressed as mean \pm SD and are representative of at least n=3 independently performed experiments.

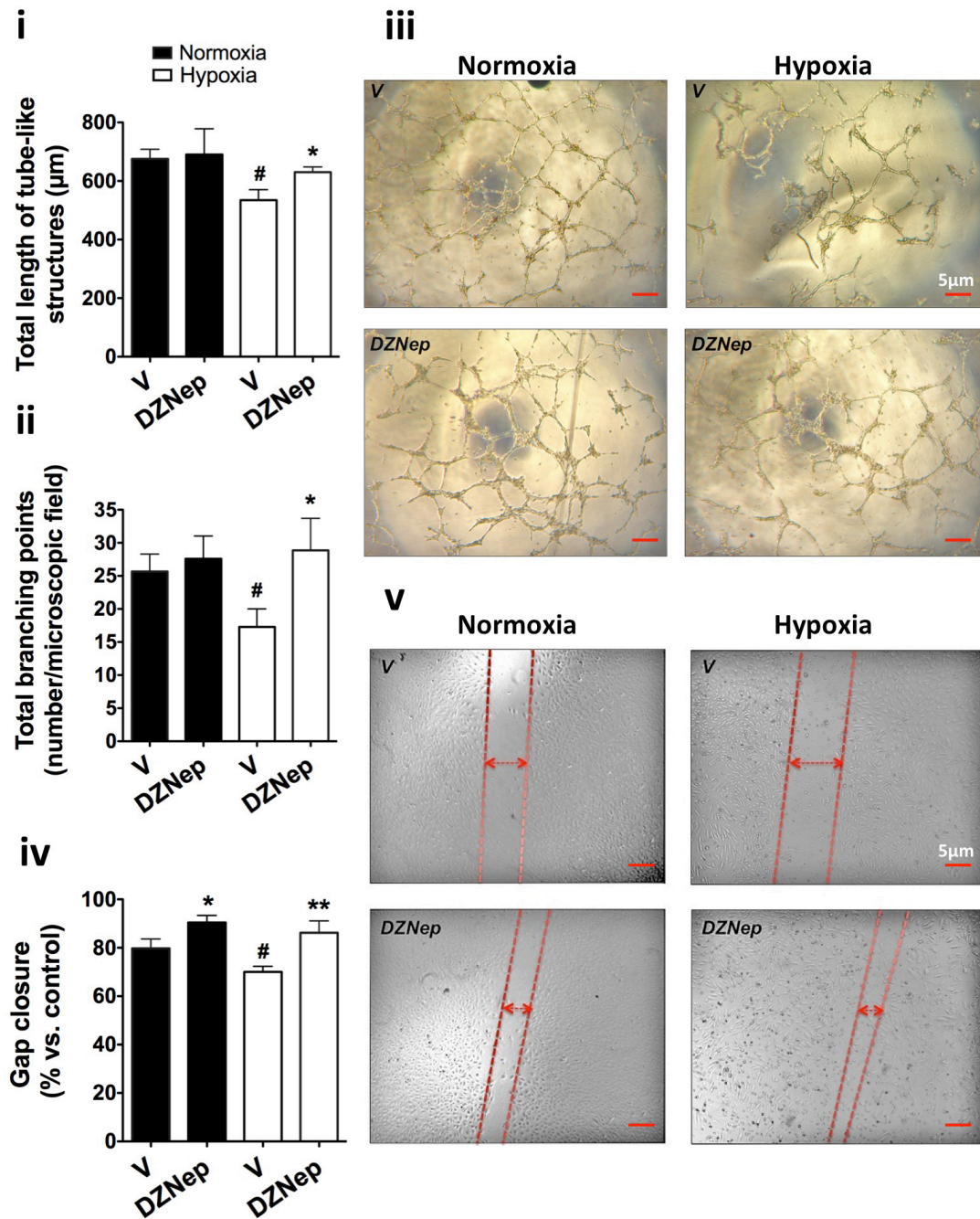


Figure S4. DZNeP increases the *in vitro* networking and migratory capacities of endothelial cells.

(i-iii): Functional properties of HUVECs treated with DZNeP or vehicle (0.1% DMSO) control were assessed using Matrigel (i-iii) and scratch (iv, v) assays. Cells were studied under normoxia or hypoxia and Matrigel (iii) and scratch (v) assay images were taken at 5X magnification. Enhanced HUVEC migration and angiogenic potential were observed under both normoxia and hypoxia in the presence of DZNeP. Scale bar: 5 µm. For the Matrigel assay, the average total length of tubes (i) and the total number of tubes branching points (ii) have been calculated. For the scratch assay, the % gap closure (iv) was calculated. All measurements are mean ± SEM. [#]p<0.05 vs. V under normoxia; ^{**}p<0.01 and ^{*}p<0.05, vs. V under hypoxia. Experiments were performed in triplicate and repeated at least three times.

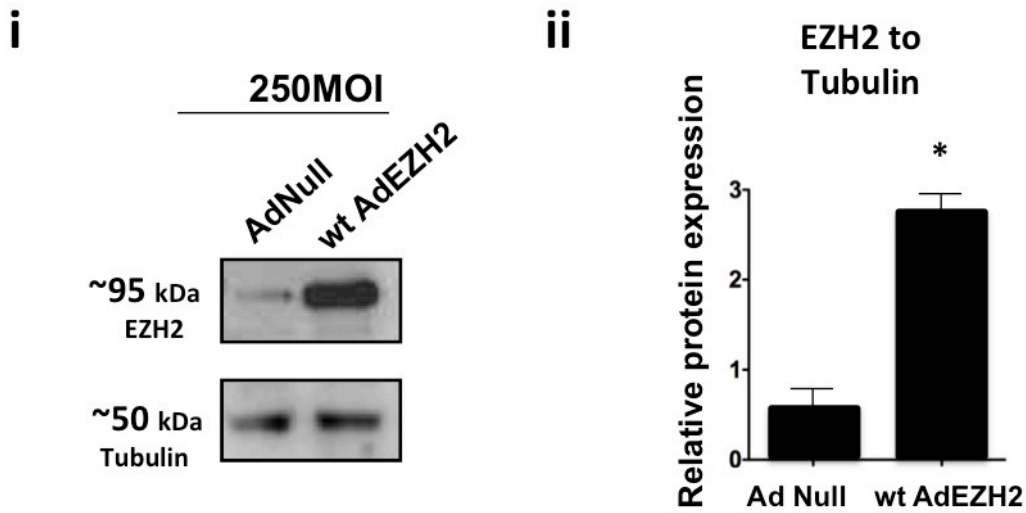


Figure S5. Overexpression of wild type EZH2 into HUVECs and quantification of Western blot analyses.

HUVECs were initially transduced overnight with Null control adenovirus (Ad Null) or wild type EZH2 (Ad wtEZH2, both at 250 M.O.I) then left in culture for further 48hours before collection of protein for Western Blot analysis (i) and further Western blot quantification (ii). Data are presented as mean \pm SEM of n=3 independent experiments. *p<0.05, vs. the respective control group (Ad Null for the wt EZH2 adenovirus).

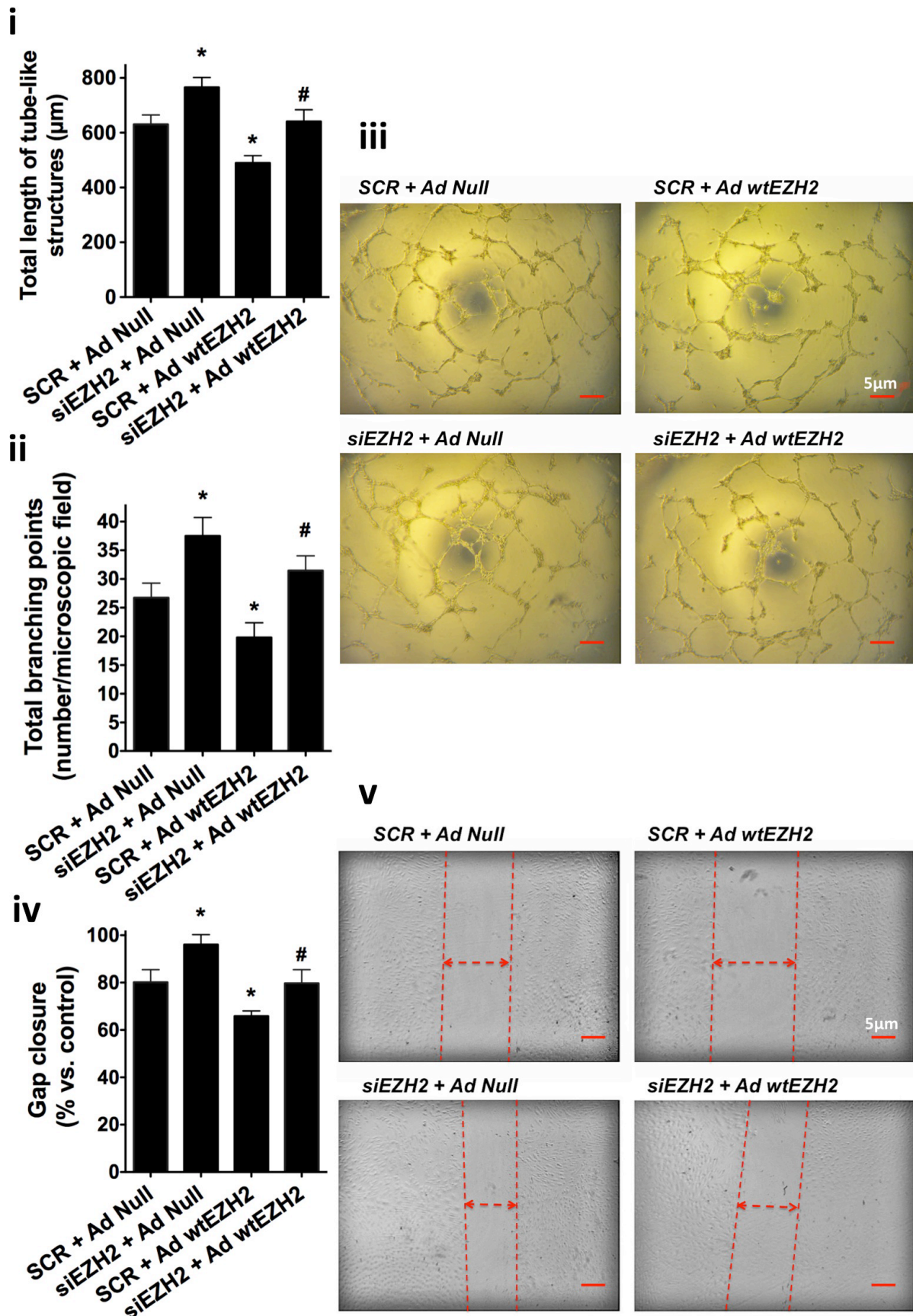


Figure S6. Rescuing the EZH2 protein levels in HUVECs worsens the endothelial cell function.

(i-iii): Functional properties of HUVECs transduced with adenovirus (Ad) wild type EZH2 (Ad wtEZH2) or Null control (Ad Null) were assessed by Matrigel **(i-iii)** and scratch **(iv, v)** assays. Upon transfection with scramble control (SCR) or siEZH2 the Matrigel **(iii top panel)** and scratch **(v top panel)** assay images were taken at 5X magnification. Cells were further transduced with AdNull or Ad wtEZH2 to rescue the expression of EZH2 protein. Further Matrigel **(iii bottom panel)** and scratch **(v bottom panel)** assay images were taken. Enhanced HUVEC migration and angiogenic potential observed under siEZH2 condition were inhibited in the presence of exogenous wtEZH2. Scale bar: 5 μ m. For the Matrigel assay, the average total length of tubes **(i)** and the total number of tubes branching points **(ii)** have been calculated. For the scratch assay, the % gap closure **(iv)** was calculated. All measurements are mean \pm SEM. # $p < 0.05$ vs. *siEZH2+AdNull*; * $p < 0.05$, vs. *SCR+Ad Null*. Experiments were performed in triplicate and repeated five times.

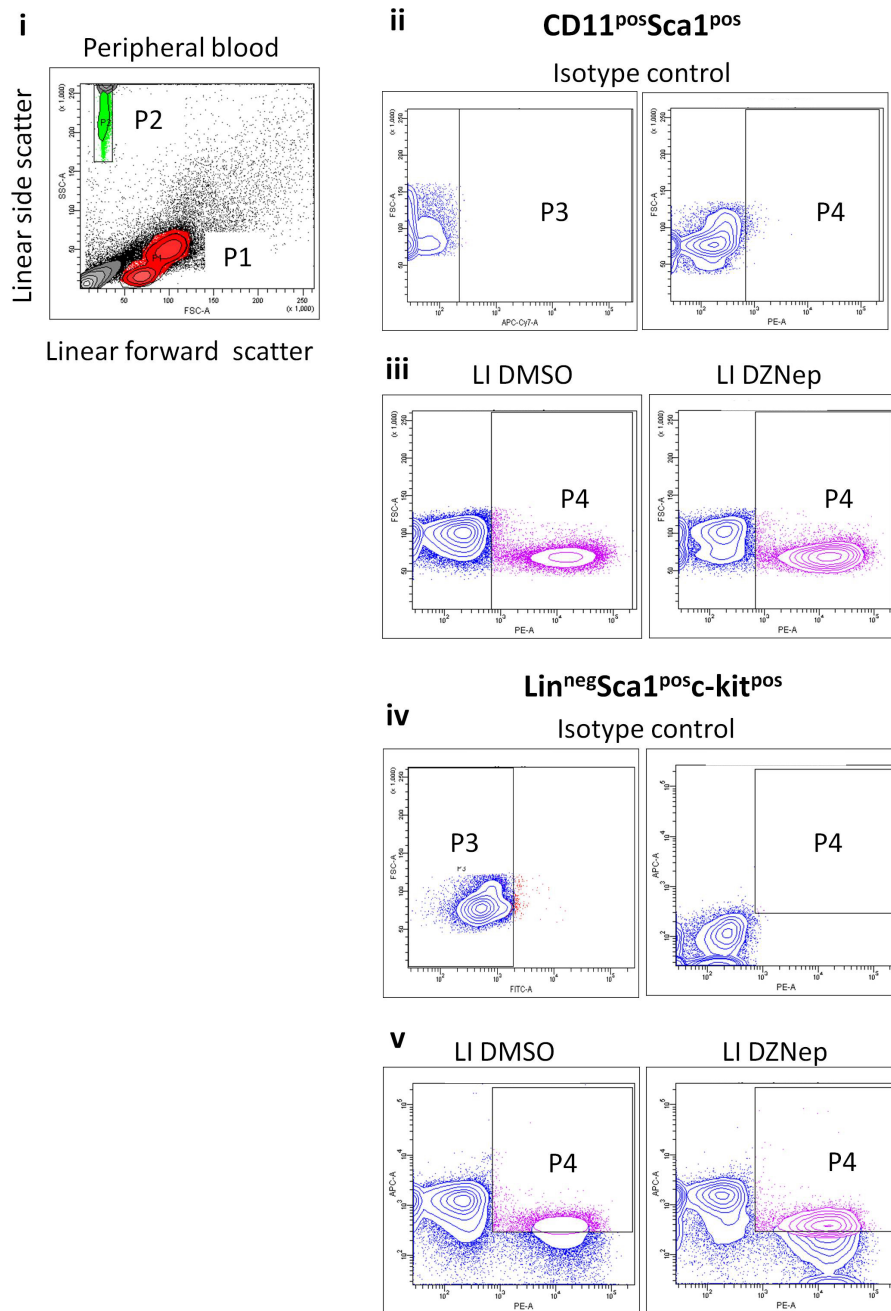


Figure S7. Flow cytometry strategies under the data presented in the Figures 7A and 7B.

Flow cytometry image representation of the total lympho-mononuclear cells from mouse peripheral blood. Forward and side scatter (i) show the total population analyzed (in red; P1). For data analysis, counting beads (green) were identified by their size (in P2 in the forward and side scatter). Identification and quantification of blood CD11b^{pos}Sca-1^{pos} and Lin^{neg}Sca-1^{pos}c-kit^{pos} cells by flow cytometry. (ii) Representative graphs show the negative control (isotype control) for CD11b^{pos} (P3) and CD11b^{pos}Sca-1^{pos} cells (P4). (iii) CD11b^{pos}Sca-1^{pos} cells (in P4, pink) in treatment group with vehicle (V) or DZNep. (iv) Representative graphs show the negative control (isotype control) for Lin^{neg} (P3) Lin^{neg}Sca-1^{pos}c-kit^{pos} (P4) (v) Lin^{neg}Sca-1^{pos}c-kit^{pos} (in P4, pink) in treatment group with vehicle (V) or DZNep. An equivalent strategy was used for the bone marrow analyzes.

Table S1. Sequence of qPCR primers used in this study.

Human gene name	Forward:	Reverse:
EZH2	CCTGAAGTATGTCGGCATCGAAAGAG	GGGCAGTGATCTCCTTCTGCAT
SUZ12	CTTACATGTCTCATCGAAACTCC	GGCTGGAAGCTCTTCATTGACA
EED	GTGACGAGAACAGCAATCCAG	TATCAGGGCGTTCAGTGTTTG
eNOS	TGATGGCGAAGCGAGTGAAG	ACTCATCCATACACAGGACCC
BDNF	GGCTTGACATCATTGGCTGAC	CATTGGGCCGAACCTTCTGGT
18S	GTAACCCGTTGAACCCCAT	CCATCCAATCGGTAGTAGCG
Mouse gene name	Forward:	Reverse:
EZH2	TTACTGCTGGCACCGTCTGATGTG	TGTCTGCTTCATCCTGAGAAATAATCTCC
SUZ12	GAAGCTGTGGAACCTCCATGTC	ACAGCATAACAGGCATGATTCATTT
EED	GCGATGGTTAGGCGATTTGAT	TTTTGCCAGGTTTCCAGCAT
eNOS	GGCTGGGTTTAGGGCTGTG	CTGAGGGTGTCGTAGGTGATG
BDNF	TCATACTTCGGTTGCATGAAGG	AGACCTCTCGAACCTGCCC
18S	GTAACCCGTTGAACCCCAT	CCATCCAATCGGTAGTAGCG

Table S2. Sequence of primer used for chromatin immunoprecipitation (ChIP) qPCR analysis in this study.

eNOS promoter region	Forward:	Reverse:
-496 to -305bp	GGGGAGGTGAAGGAGAGAACC	GAGCCACCAGGGGGTCATAA
-493 to -301bp	CCAGGAGTTCTTGTATGTATGG	GGTCCTTCTGTGATGTGGC
-347 to -114bp	GGTGCCACATCACAGAAGGA	CACAATGGGACAGGAACAAGC
-318 to -208bp	GGTGCCACATCACAGAAGG	AGCCCAGGTGTCCAGCA
-220 to +19bp	AGTCCTCACAGCGGAACC	ACTGTGCGTCCACTCTGC
-7 to +171bp	AGCAGGCAGCAGAGTGGAC	GGCCCTTACCTGTGTTCTG
BDNF promoter region	Forward:	Reverse:
-814 to -610bp	GCTTTTAAAGGGCGACACAG	ACAGAGCCAACGGATTTGTC
-775 to -581bp	TGCTTTCAGCCAGATGTCTC	GAGTTGGTCCCTCTGTTGC
-753 to -480bp	CACAGGGAGATGCAAGTTGA	GAAAGGCACTCCCATTTCAG
-510 to -220bp	GCGCTGAATTTTGATTCTGG	GAAAGTGGGTGGGAGTCCA
-260 to -82bp	AACGCACACACACAGAAAGC	CCCTCCTCCTGAAATTGTGA
-113 to +20bp	GCTTTTAAAGGGCGACACAG	ACAGAGCCAACGGATTTGTC
Control primers promoters:	Forward:	Reverse:
MYT-1	ACAAAGGCAGATACCCAACG	GCAGTTTCAAAAAGCCATCC
Neuogenin D2	TCACAGGGCCAAGATAAAGC	AAGAGCGAGCATCTGTTTCC
GAPDH	CGGGATTGTCTGCCCTAATTAT	GCACGGAAGGTCACGATGT

Table S3. Antibodies used in the study.

Antibody	Application	Source	Cat No:
Rb - EZH2	WB	Active Motif	39933
Ms - EZH2 (clone AC22)	ChIP	Millipore	17-662
Rb - SUZ12	WB, ChIP	Abcam	ab12073
Rb - EED	WB, ChIP	Santa Cruz Biotechnology	sc-28701
Rb - H3K27me3	WB, ChIP	Millipore	07-449
Rb - H3K27me2	WB, ChIP	Millipore	07-452
Rb - H3K4me3	WB, ChIP	Millipore	07-473
Rb - H3KAc	WB, ChIP	Millipore	06-599
Rb - H3 total	WB, ChIP	Active Motif	39163
Rb - eNOS	WB	Cell signaling	9572
Ms - BDNF	WB, ELISA	Promega	G164B
Rb - YY1 (C-20)	WB, ChIP	Santa Cruz Biotechnology	sc-281
Rb - RNA Polymerase II (N-20)	WB, ChIP	Santa Cruz Biotechnology	sc-899X
Rb - IgG control	ChIP	Millipore	06-489
Ms - IgG control	ChIP	Millipore	12-371B
Ms - Tubulin	WB	Cell Signaling	2148S
Ms - Lamin A/C	WB	Active Motif	39287

